Available online at www.sciencedirect.com
ScienceDirect
Journal of Power Sources 163 (2006) 616–622
JOURNAL OF POWER SOURCES
www.elsevier.com/locate/jpowsour

A modified activated carbon aerogel for high-energy storage in electric double layer capacitors

Baizeng Fang *, Leo Binder

Institute for Chemical Technology of Inorganic Materials, Graz University of Technology, Stremayrgasse 16/III, A-8010 Graz, Austria

Received 19 July 2006; received in revised form 12 September 2006; accepted 12 September 2006
Available online 27 October 2006

Abstract

A novel electrode material, modified activated carbon aerogel, produced by grafting a vinyltrimethoxysilane (vtmos) functional group on the surface of activated carbon aerogel (ACA), has been developed for high-energy storage in electric double layer capacitor (EDLC). Surface modification with surfactant vtmos enhances the hydrophobicity of ACA and its affinity to propylene carbonate (PC) solvent, which improves the wettability of ACA in a PC-based electrolyte solution, resulting in not only a lower resistance to the transport of electrolyte ions within ACA micropores but also more accessible surface area for the formation of an electric double layer, and accordingly, higher specific capacitance and energy density.

Keywords: Carbon aerogel; Activation; Surface treatment; Infrared spectroscopy; Electrochemical properties

1. Introduction

The ultimate energy storage device should have high energy density that can be released rapidly. First generation supercapacitors also referred to as ultracapacitors and electrochemical double layer capacitors (EDLC), have relatively high energy density but also very high equivalent series resistance and are therefore only used in very low power memory backup applications. To develop supercapacitors with high energy density and power capability lots of electrode materials have been examined. Though supercapacitors employing metal oxides [1] or conducting polymers [2] have been increasingly investigated, carbon–carbon supercapacitors remain the most extensively studied and least expensive technology. Various carbonaceous materials such as activated carbons [3], aerogels [4], xerogels [5], templated carbons [6], nanotubes [7,8] and carbide-derived carbons (CDCs) [9] have been studied extensively as electrodes for supercapacitors. Amongst carbonaceous materials, carbon aerogels represent promising EDLC materials because of their attractive properties such as high electrical conductivity, controllable pore structure and relatively high useable surface area for electric double-layer (EDL) formation [10–14]. However, carbon aerogels conventionally prepared provide predominantly mesopores, resulting in a relatively small surface area for EDL formation in comparison with microporous carbons, i.e., activated carbon. Without change of the skeletal carbon gel structure, production of micropores by activation of carbon aerogel, giving a unique carbon material with a bimodal pore structure could increase the useable surface area for EDL formation and accordingly the capacitance considerably at relatively low charge/discharge rates [12]. However, at a high discharge rate the energy available from the capacitor using activated carbon aerogel (ACA) electrodes becomes lower than that of original carbon aerogel, which is primarily attributable to the narrowing of mesopores, hindering fast transport of electrolyte ions within micropores, and to poor wettability of the electrodes in electrolyte solution, resulting in a small accessible surface area for EDL formation and a high internal resistance. To improve wettability of the electrodes in electrolyte solution especially non-aqueous electrolyte solutions, we modified carbonaceous materials with surfactant sodium oleate (OAS) [16]. Experimental results have shown that wettability of the carbon electrodes in electrolyte solution based on propylene carbonate (PC) solvent can be improved by the

* Corresponding author. Fax: +43 316 8738272.
E-mail address: baizengfang@163.com (B. Fang).

0378-7753/$ – see front matter © 2006 Elsevier B.V. All rights reserved.
doi:10.1016/j.jpowsour.2006.09.014

attachment of hydrophobic moiety of surfactant sodium oleate (OAS), resulting in enhanced performance of EDLCs [15–17]. However, the improvement in the performance of EDLCs by surface modification with OAS is relatively limited, primarily attributable to the limited enhancement in the hydrophobisation of carbon due to the existence of remaining hydrophilic functional groups (i.e., hydroxyl) after the modification. Therefore, further enhancement in hydrophobisation of carbon is necessary to improve the wettability of carbon in PC solvent. Recently, we have paid more attention to surfactant vinyltrimethoxysilane (vtmos), which can enhance greatly hydrophobisation of carbon materials by grafting of vtmos functional groups [18]. We have conducted extensive investigation onto effects of this surfactant, and found that better EDLC performance (high specific capacitance, energy density and power capability) can be expected from the vtmos-modified carbon than from OAS-modified one. Here we report the details of surface modification of ACA with surfactant vtmos and the excellent EDLC performance obtained from vtmos-modified ACA (MACA).

2. Experimental

2.1. Synthesis and activation of carbon aerogel

Carbon aerogel was derived from pyrolysis of a resorcinol–formaldehyde (RF) gel according to a method proposed by Pekala [10]. Upon preparation of a RF gel, the mass percentage of the reactants in solution was set at RF = 20% and the molar ratio of resorcinol (R) to catalyst Na_2CO_3 (C) was set at R/C = 150. The molar ratio of formaldehyde to resorcinol was held at a constant value of 2.

After weighing out the required amounts of each component, the components were combined in a glass tube (40 ml in capacity) and the resulting solution briefly stirred. To avoid sedimentation of RF polymers in the solution, the initial pH of RF solution was adjusted to 6.5–7.4 by addition of a few drops of 1 M NaOH solution. The RF solution was treated with a standard gelation/aging cycle $t_1/t_2/t_3$ of 1/1/1 (where t_{1-3} denotes the days at 25 °C, 50 °C and 90 °C, respectively). The gelation/aging cycle was accomplished by placing the glass tube containing the reactants into an oven for which the temperature was adjusted over several days. To accomplish this, the tube was placed into a sealed glass beaker containing a few milliliters of distilled water to provide a saturated humidity environment, which prevented water evaporation during the gelation/aging cycle. At the end of this process, the monomers were converted into the RF gel, which existed as a dark red, soft and porous solid. After the gelation/aging cycle was completed, the resulting gel cylinder was removed from the glass tube and then wrapped with a piece of cheese cloth and tightened with nylon twine for protection from cracking during the solvent exchange steps. Next, the wrapped gel cylinder was suspended in an agitated bath of 0.125 wt.% trifluoroacetic acid in water at 45 °C for 3 days to stop the polycondensation process and to extend the cross-linking between the resorcinol and formaldehyde in the gel. Then, the trifluoroacetic acid solution-filled gel was treated with pure acetone in an agitated bath for 4 days at 45 °C to replace the trifluoroacetic acid solution with acetone as the pore liquid. The acetone bath was exchanged daily to remove the residual trifluoroacetic acid and water that had entered the bath during the solvent exchange process. The acetone-filled RF gel was then dried with microwave oven at 500 W for 10 min prior to carbonization. Pyrolysis of the dried RF gel was carried out under a flow of pure N_2 gas. The heating profile was as follows: heating from room temperature to 250 °C at a rate of 2 °C min^{-1}, holding this temperature for 4 h, and then raising temperature to 1000 °C at the same heating rate, holding this temperature for 4 h and then cooling down to room temperature by turning off the furnace.

Activated carbon aerogel was prepared by carbonization of carbon aerogel with KOH at 900 °C for 4 h. The heating profile was the same as that for synthesis of carbon aerogel. The mass ratio of KOH to carbon aerogel was set as 3:1. After activation the carbon aerogel was washed with deionised water till the pH value reached ca. 7.

2.2. Surface modification of carbon aerogel and activated carbon aerogel

Surface modification of carbon aerogel (CA) or activated CA (ACA) with surfactant vtmos was performed as follows. Two grams of CA (or ACA) was soaked by 20 ml of surfactant (vtmos) aqueous solution (0.25 wt.%) and shaken for 12 h at 25 °C. After filtration, the carbon slurry was dried at 120 °C under vacuum for 24 h.

2.3. Fabrication of carbon electrodes and construction of test capacitors

The fabrication of carbon electrodes was as follows. Carbon aerogel (active material), graphite powder (conductivity enhancing material), polytetrafluoroethylene (PTFE, binder) and carboxymethylcellulose (CMC, auxiliary binder) were mixed in a mass ratio of 90:4:4:2 and dispersed in deionised water (the mass ratio of carbon to water was set as 1:3). After stirring for several hours (typically 3 h), the slurry was cast onto an Al foil (as a current collector, 30 μm in thickness) with an applicator. The carbon coated Al foil was then dried under vacuum at 120 °C for ca. 12 h, and punched in required size (16 mm in diameter) as electrodes. Apparent surface area of the electrode was ca. 2 cm^2 and thickness was about 150 μm. Mass of active material in the carbon electrode was ca. 4 mg. Test capacitors were constructed in a glove box. A separator Celgard 3400 soaked with 200 μl non-aqueous electrolyte solution (1 M Et_4NBF_4–PC) was sandwiched between two carbon electrodes.

2.4. Characterization of carbon aerogels and test capacitors

The surface area and pore-size distribution of CA and ACA were calculated from nitrogen adsorption isotherms at 77 K (Micromeritics ASAP2010) using the Brunauer, Emmett and Teller (BET), and Barrett, Joyner and Halenda (BJH) methods,

respectively. CA and ACA were also characterized by Fourier transform infrared (FT-IR) spectrum, which was recorded on a FT-IR spectrometer (FT-IR-6200, PS-4000, JASCO). Each of the IR spectra was the average of 32 scans at a speed of 2 s per scan. The resolution of the spectrometer was set to 4 cm^{-1}.

For all electrochemical measurements, one electrode of the capacitor was used as the positive electrode and the other one as the negative electrode. Electrochemical impedance spectroscopy measurements were carried out in the range of 100 kHz to 10 mHz with ac amplitude of 10 mV and dc potential of 100 mV.

For constant-current charge–discharge tests, a battery test system (Maccor Inc., USA) was employed, and a voltage range of 0.05–3.0 V was set. Current density for charging was set at 3 mA cm^{-2} in all cases. Discharge capacitance (C) of a capacitor was obtained by integration of the constant-current discharge curve. Specific capacitance of electrode material was defined as electrode capacitance per unit mass active material in the electrode. Energy delivered to a load (E_{load}) by a capacitor was calculated according to the formula $E_{load} = (1/2)C[(V_{initial} - IR)^2 - V_{final}{}^2]$, where $V_{initial}$, V_{final}, I and R stands for the initial voltage limit, final voltage limit, discharge current and direct current internal resistance of a discharge process, respectively. Specific energy of a capacitor was defined as the energy delivered to a load (i.e., E_{load}) divided by total mass of the active material in two electrodes. IR drop was collected at the beginning of a discharge process.

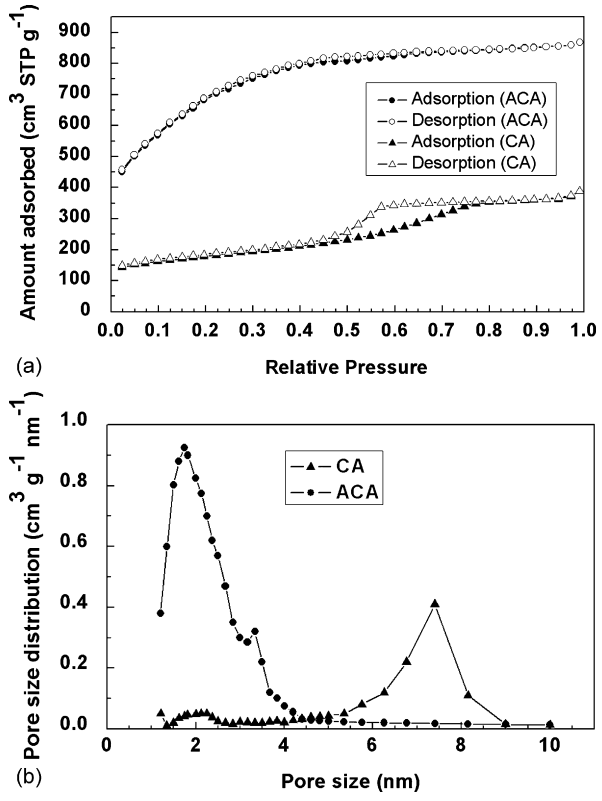

Fig. 1. N_2 adsorption–desorption isotherms at 77 K (a) and pore-size distribution (b) for the carbon aerogel (CA) and for the activated CA (ACA).

3. Results and discussion

3.1. Surface characterization of carbon aerogel and activated carbon aerogel

Fig. 1 shows N_2 adsorption–desorption isotherms at 77 K (Fig. 1a) and pore-size distribution (Fig. 1b) for carbon aerogel (CA) and activated carbon aerogel (ACA).

The N_2 adsorption–desorption isotherms for CA show significant hysteresis characteristic of mesopores at high relative pressure (higher than 0.4). On the other hand, the N_2 adsorption–desorption isotherms for ACA show a large adsorption capacity at relative pressures of 0.1–0.4, indicating that large quantity of micropores have been introduced into carbon aerogel after the activation. In addition, at relative pressures higher than 0.4 neither evident hysteresis characteristic of mesopores nor marked increase in adsorption capacity was observed for the ACA, suggesting that most of mesopores in CA have been converted into micropores after the activation. It is evident from Fig. 1b that ACA exhibits a bimodal pore size distribution, one dominant peak centres at 1.7 nm and another peak centres at 3.3 nm while predominant peak centres at 7.5 nm for CA.

Table 1 summarizes data obtained from BET measurements for the CA and ACA. It is clear that there are only small amount of micropores in CA. After activation, lots of micropores have been produced, and BET surface area of carbon aerogel increased considerably.

3.2. Performance of the test capacitors based on various carbon aerogels

Fig. 2 shows the ratios of specific capacitance (F g^{-1}) or specific energy (Wh kg^{-1}) for the capacitor using ACA electrodes to that of the capacitor using CA electrodes at various discharge rates.

It is clear that both the specific capacitance and energy for the ACA-capacitor are greater than ones obtained from CA-capacitor at relatively low discharge rate, i.e., at 3 mA cm^{-2}, about 2.5 times of specific capacitance and energy are available from the former, which are primarily attributable to higher specific surface area of the ACA. However, the ratio of specific capacitance, especially the ratio of specific energy decreases sharply with the increasing discharge rates and at 48 mA cm^{-2}, the specific energy available from the ACA-capacitor is lower than that from CA-capacitor. The reasons can be explained as follows. After the activation, lots of micropores have been intro-

Table 1
Specific surface area and pore volume for the original carbon aerogel (CA) and activated carbon aerogel (ACA)

Material	BET surface area (m^2 g^{-1})	Micropore volume (cm^3 g^{-1})	Mesopore volume (cm^3 g^{-1})
Carbon aerogel (CA)	592	0.25	0.43
Activated CA (ACA)	2371	1.03	0.32

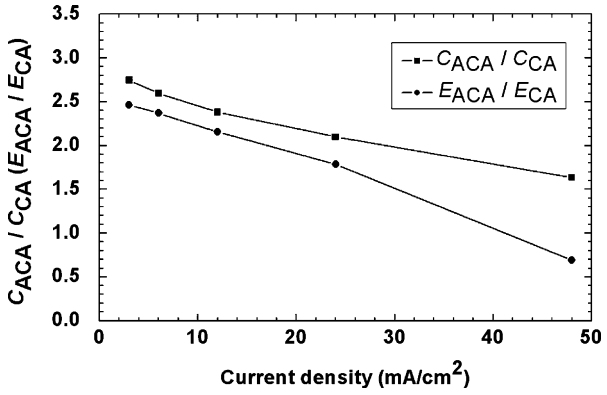

Fig. 2. Ratios of specific capacitance ($F g^{-1}$) or energy delivered ($Wh kg^{-1}$) at various discharge rates of the capacitor using ACA electrodes to that of the capacitor using CA electrodes.

duced into carbon aerogel. The content of mesopores in the carbon aerogel decreases and some mesopores become narrowed, hindering fast transport of the electrolyte ions and resulting in decreased surface area for EDL formation and increased internal resistance. This situation becomes especially conspicuous at high discharge rates. Due to the marked decrease in the useable surface area, the specific capacitance, and accordingly the specific energy decrease dramatically. In addition, the increase in the internal resistance resulted in a further energy loss.

To improve the performance of ACA-capacitor, surface modification of ACA was conducted with 0.25 wt.% surfactant vtmos aqueous solution.

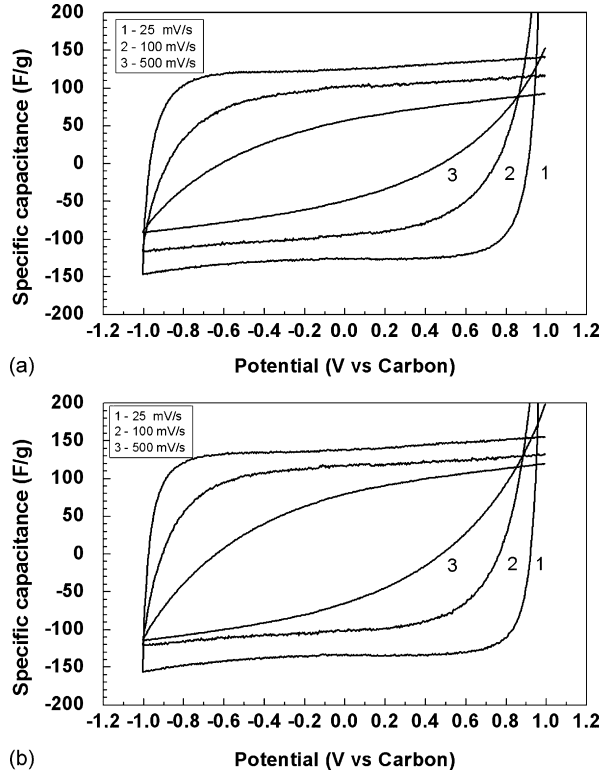

Fig. 3. Cyclic voltammograms at various scan rates for the capacitors using ACA (a) or MACA (b) as electrodes, where the current has been converted into specific capacitance based on the mass of active material of 4 mg.

Fig. 3 shows cyclic voltammograms at various scan rates for the capacitors using ACA or MACA as electrodes, respectively, where the current has been transferred into the specific capacitance based on the mass (4 mg) of active material in one electrode. For an ideal supercapacitor, its capacitance is independent of frequency, so the charge stored by a capacitor is proportional to the voltage imposed. Therefore, in the case of the CV measurements, for a constant sweep rate ($mV s^{-1}$), the current response will stay constant. At the same scan rate, more ideal capacitive behaviour was observed for MACA with a steeper current change at the switching potentials (−1.0 and 1.0 V), resulting in a more rectangular-shaped *i*–*V* curve. The slower changes at the switching potentials in the cyclic voltammogram of ACA stem from the slower reorganization of the double layer owing to slower ionic motions in micropores.

In addition, higher capacitances were obtained from MACA at all the applied scan rates, suggesting that after the modification more surface area of the carbon was accessible to the electrolyte ions due to the improved wettability of carbon and more quick charge propagation.

The improvement in hydrophobisation of ACA improves the affinity of the carbon surface to non-polar organic solvent, propylene carbonate (PC), and accordingly improves the wettability of the electrodes.

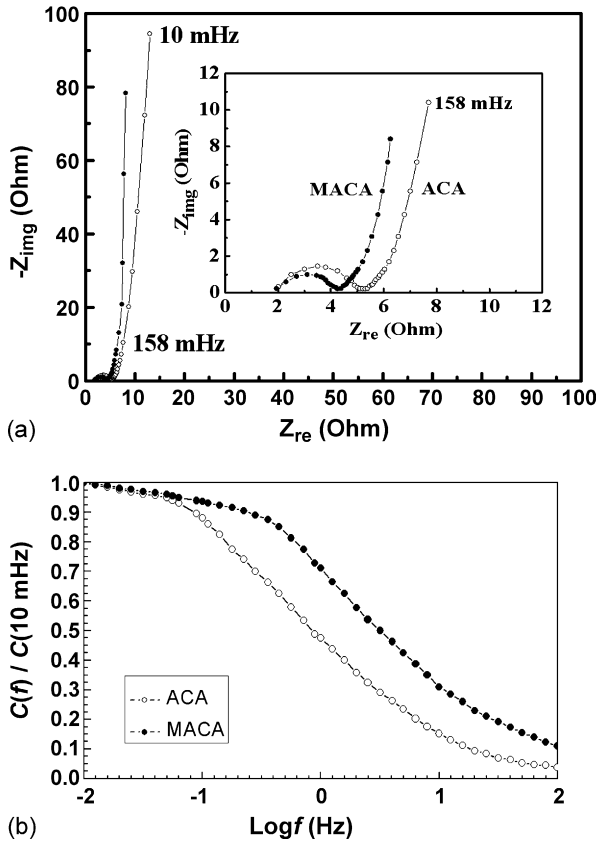

Fig. 4. Nyquist plots (a) for capacitors based on ACA or MACA electrodes in the frequency range of 100 kHz to 10 mHz (the inset shows the expanded high frequency region of the plot) and the frequency-dependent capacitances (b) normalized to the lowest frequency (10 mHz).

Fig. 4a shows Nyquist plots for the capacitors using ACA or MACA as electrode material, respectively. A depressed semicircle was observed in the high frequency region (between 100 kHz and 400 Hz), which represents a parallel combination of resistive and capacitive components. Electrolyte resistance was estimated around 2 Ω from the crossover point of the highest frequency with the real part of the impedance. Ionic resistance was estimated ca. 2.2 and 3.2 Ω from the diameter of the semicircle for MACA and ACA electrode, respectively. The lower resistance for MACA is probably attributable to more rapid mass transport within micropores of porous carbon due to the improved wettability of active material. At low frequency (lower than 400 Hz), the imaginary part of the impedance increases, showing the capacitive behaviour of the supercapacitor.

For further investigation on performance of the capacitors based on various carbon aerogels electrodes, *RC* time constant (*R* and *C* denote the equivalent series resistance (ESR) and capacitance, respectively.) were derived and compared for various carbon aerogels. It is well known that if any capacitor has a large *RC* time constant, the rate capability is poor. In order to compare the *RC* time constant for the capacitors using various carbon aerogel electrodes, the frequency-dependent capacitance was obtained in low-frequency region according to $C(f) = 1/(i2\pi fZ(f))$, where i, f and $Z(f)$ are the imaginary unit, ac frequency and complex impedance at a frequency, respectively.

The frequency-dependent capacitances of the capacitors using ACA electrodes or MACA electrodes, normalized to the lowest frequency (10 mHz) values are shown in Fig. 4b.

The frequency-dependent capacitance of porous electrodes can be analyzed using the transmission line model, which was proposed by De Levie with an assumption that pores are uniform and cylindrical [19]. The parameter 'penetration depth', $l = 1/(\pi fR'C')^{1/2}$, is useful to understand the impedance behaviour of porous electrodes, where R' and C' represent the pore resistance and pore capacitance per unit pore length, respectively. It is clear that when the ac frequency is sufficiently high for the penetration depth (l) to be smaller than the pore length (l_p) of porous electrodes, only the outer surface (near pore opening) is influenced by the ac voltage signal, and as a result, a small capacitance is observed because only a limited part of electrode surface is utilized for the formation of electric double layer. In the low-frequency extreme, where the condition $l > l_p$ holds, most of the pore surface is utilized and results in a maximum capacitance. In the intermediate-frequency region, a monotonous capacitance change is observed.

The *RC* time constant can be compared for the capacitors using various carbon aerogel electrodes by analyzing the capacitance profiles in the intermediate-frequency region, where the cutoff frequency is taken as the frequency at which the capacitance is 50% the value at the lowest frequency (10 mHz). The relative $R'C'$ values are extracted at the cutoff frequency using the above equation with the penetration depth (l) being assumed to be the same for the two carbon aerogel materials. The cutoff frequencies are 0.8 and 3.16 Hz for ACA and MACA, respectively, and the *RC* time constants of the ACA-capacitor are calculated as 3.95 times that of MACA-capacitor, which indicates that after the surface modification the power capability of

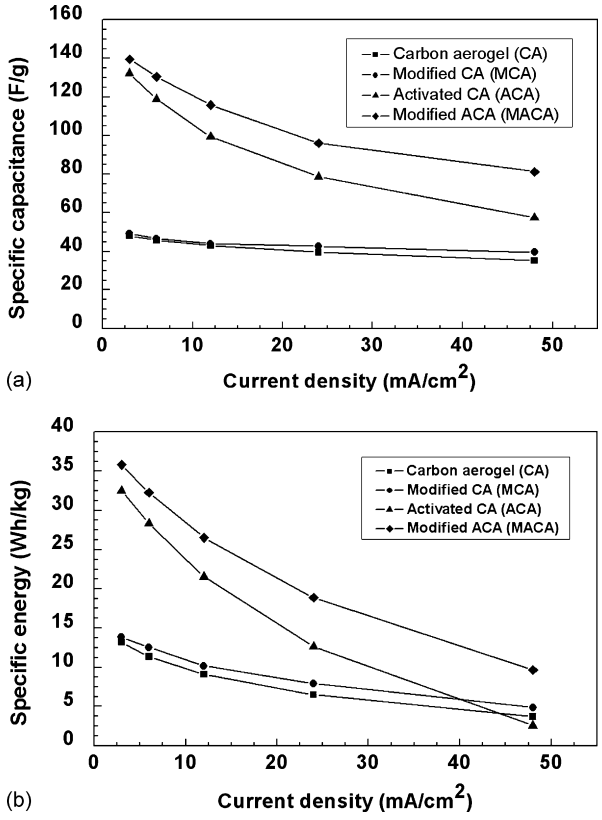

Fig. 5. Specific capacitance (a) and energy density (b) at various discharge rates for the capacitors using various carbon aerogel materials.

ACA-capacitor has been improved greatly. This conclusion is consistent with that drawn from the CV tests.

Fig. 5 shows specific capacitance and specific energy obtained at various discharge rates for the various carbon aerogels. For comparison data obtained from original CA and modified CA (MCA) are also displayed. It is clear from Fig. 5a that with increasing discharge rate the specific capacitances decrease for all carbon materials, which is attributable to the decreased sites for EDL formation. Higher capacitance and slower decrease in the capacitance with increasing discharge rate were observed for the vtmos-modified carbons, suggesting more rapid ions transport for the modified materials under the same condition. A similar tendency was observed for the energy density at various discharge rates as shown in Fig. 5b, i.e., higher specific energy and slower decrease in the specific energy were achieved by the modified carbon material. In comparison with specific capacitance shown in Fig. 5a, the specific energy has a more noticeable decrease with increasing discharge rates due to additional effects from the polarization resistance, which becomes a primary source for the energy loss at a high discharge rate. The enhancement in capacitance and specific energy after surface modification is primarily attributed to the improvement in wettability of the electrode material, resulting in more usable sites for EDL formation, and lower internal resistance, resulting in less energy loss.

To confirm that improved EDLC performance of carbon materials is attributable to their improved wettability in PC solvent, resulting from the enhanced hydrophobisation of car-

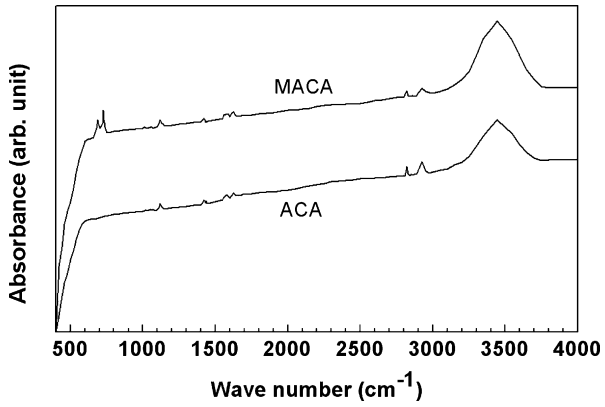

Fig. 6. FT-IR spectra for the activated carbon aerogel (ACA) and vtmos-modified ACA (MACA).

bon materials due to the attached organic functional groups ($-(CH_3O)_2SiCH{=}CH_2$), FT-IR spectroscopy was conducted. It was found in Fig. 6 that the spectrum of MACA comprises two small bands at 728 cm^{-1} and 691 cm^{-1}, not observed for ACA. In addition, the characteristic bands of vtmos were not observed in the spectrum of MACA suggesting that the organosilicon compound was not adsorbed. The two small peaks at 728 cm^{-1} and 691 cm^{-1} could correspond to those shifted, of vtmos, usually occurring at 773 cm^{-1} and 817 cm^{-1}, which are attributable to the vibrations of Si–O bonds and Si–C ones within the group $Si–CH{=}CH_2$, respectively. Such a shift of the peaks toward lower wave numbers may account for a possible increase of the rigidity of the molecule, induced by the grafting [18].

Various grafting possibilities of the vtmos may be conjectured. In a silylation reaction, water induces the hydrolysis of the alkoxysilane molecules, which can next condense with the hydroxyl groups already present. Depending on the surface density of the latter, the binding of the vtmos to the carbon surface may be achieved through one, two or three bridging hydroxyls [18,20,21]. The mechanism for grafting needs further investigation in the future.

Grafting of vtmos functional groups improves the hydrophobisation of carbon and the affinity of the carbon material towards non-polar organic solvent, propylene carbonate (PC) and accordingly improves the wettability of carbon in PC-based electrolyte, facilitating the electrolyte ions to access micropores of porous carbon.

For the modified carbon, the enhancement in capacitance is primarily attributed to the improvements of the wettability, which provides more accessible surface area for EDL formation. The improvement in specific energy is attributed to the increase in capacitance and attributed to the decrease in IR drop. From the expression for energy to a load (E_{load}), $E_{load} = (1/2)C[(V_{initial} - IR)^2 - V_{final}{}^2]$, it is clear that IR drop plays a very important role in energy delivery especially at a high discharge rate. The improvement in the wettability of electrode material lowers energy loss (i.e., the energy dissipated by a capacitor itself) by lowering the internal resistance.

In comparison with the results obtained from OAS-modified ACA at the same discharge rate (i.e., 48 mA cm^{-2}, 38% of enhancement in capacitance and 72% of enhancement in energy density) [17], better EDLC performance has been realized by vtmos-modified ACA (i.e., 41% of enhancement in capacitance and 274% of enhancement in energy density), which is probably attributable to better hydrophobisation of vtmos-modified ACA, resulting from the replacement of larger amount of hydrophilic hydroxyl by hydrophobic vtmos functional groups.

4. Conclusions

In this study, a novel carbon aerogel electrode material, modified activated carbon aerogel (MACA), was developed by grafting of vtmos functional group on the surface of activated carbon aerogel (ACA) for enhanced electric energy storage in EDLC. Activation of carbon aerogel enhances its specific surface area considerably and thus improves its specific capacitance greatly at relatively low charge–discharge rates. However, narrower pore size and poor wettability to electrolyte solution restrict ACA greatly from large-current applications. Grafting of vtmos functional groups on the surface of ACA enhances its hydrophobisation and affinity toward propylene carbonate (PC) solvent, and thus improves its wettability in PC-based electrolyte. The improved wettability results in not only a lower resistance to the transport of electrolyte ions within micropores of MACA electrode but also more usable surface area for EDL formation, and accordingly, higher specific capacitance, specific energy and power capability available from the MACA-based capacitor. The effects from the surface modification become more pronounced at higher discharge rate, i.e., 48 mA cm^{-2}, at which about four times of specific energy and power capability (estimated from the *RC* time constants) of ACA can be achieved from MACA, suggesting that MACA is a novel and very promising electrode material for highly improved EDLC performance.

Acknowledgments

This work was financed by FWF, the Austrian Science Research Foundation, Lise Meitner Programme, Austria. We thank our colleague Prof. O. Fruhwirth for synthesis of carbon aerogel and activated carbon aerogel, thank Dr. Wolfram Kohs for BET measurements of the carbon aerogel materials, and thank Mr. Fridtjof Lechhart at Daramic, LLC in Germany for providing porous membrane material, Celgard 3400.

References

[1] B.E. Conway, Electrochemical Supercapacitors—Scientific Fundamentals and Technological Applications, Kluwer Academic/Plenum, New York, 1999.
[2] M. Mastragostino, C. Arbizzani, F. Soavi, J. Power Sources 97–98 (2001) 812–815.
[3] M. Endo, Y.J. Kim, K. Osawa, K. Ishii, T. Inoue, T. Nomura, et al., Electrochem. Solid State Lett. 6 (2003) A23–A26.
[4] R. Saliger, U. Fischer, C. Herta, J. Fricke, J. Non-Cryst. Solids 225 (1998) 81–85.
[5] C. Lin, J.A. Ritter, Carbon 38 (2000) 849–861.
[6] A.B. Fuertes, F. Pico, J.M. Rojo, J. Power Sources 133 (2) (2004) 329.

[7] E. Frackowiak, S. Delpeux, K. Jurewicz, K. Szostak, D. Cazorla-Amoros, F. Beguin, Chem. Phys. Lett. 361 (2002) 35–41.
[8] E. Frackowiak, K. Jurewicz, S. Depleux, F. Beguin, J. Power Sources 97–98 (2001) 822–825.
[9] E. Lust, A. Janes, M. Arulepp, J. Electroanal. Chem. 562 (1) (2003) 33–42.
[10] R.W. Pekala, J. Mater. Sci. 24 (1989) 3221–3227.
[11] H. Probstle, C. Schmitt, J. Fricke, J. Power Sources 105 (2002) 189–194.
[12] Y. Hanzawa, K. Kaneko, R.W. Pekala, M.S. Dresselhaus, Langmuir 12 (1996) 6167–6169.
[13] R. Saliger, V. Bock, R. Petricevic, T. Tillotson, S. Geis, J. Fricke, J. Non-Cryst. Solids 221 (1997) 144–150.
[14] R. Petricevic, G. Reichenauer, V. Bock, E. Emmerlin, J. Fricke, J. Non-Cryst. Solids 225 (1998) 41–45.
[15] B. Fang, Y.Z. Wei, K. Suzuki, M. Kumagai, Electrochim. Acta 50 (2005) 3616–3621.
[16] B. Fang, Y.Z. Wei, K. Maruyama, M. Kumagai, J. Appl. Electrochem. 35 (2005) 229–233.
[17] Y.Z. Wei, B. Fang, S. Iwasa, M. Kumagai, J. Power Sources 141 (2005) 386–391.
[18] F. Cosnier, A. Celzard, G. Furdin, D. Begin, J.F. Mareche, O. Barres, Carbon 43 (2005) 2554–2613.
[19] R. De Levie, in: P. Delahay (Ed.), Advances in Electrochemistry and Electrochemical Engineering, vol. 6, Interscience Publishers, New York, 1967, p. 329.
[20] D. Derouet, S. Forgeard, J.C. Brosse, J. Emery, J.Y. Buzare, J. Polym. Sci. Polym. Chem. 36 (3) (1998) 437.
[21] W. Yoshida, R.P. Castro, J.D. Jou, Y. Cohen, Langmuir 17 (19) (2001) 5882–5888.